Thermochimica Acta 490 (2009) 1–7

Contents lists available at ScienceDirect

Thermochimica Acta

journal homepage: www.elsevier.com/locate/tca

Enhanced accuracy in a silicon-nitride-membrane-based microcalorimeter with variation of lateral layout

Ki Sung Suh, Jae Wook Kim, Hyung Joon Kim, Yun Daniel Park, Kee Hoon Kim*

CSCMR and FPRD, Department of Physics and Astronomy, Seoul National University, Seoul 151-747, South Korea

ARTICLE INFO

Article history:
Received 28 May 2008
Received in revised form
22 November 2008
Accepted 26 November 2008
Available online 3 December 2008

Keywords:
Heat capacity
Silicone-nitride membrane
Microcalorimeter
Relaxation method

ABSTRACT

We report the effect of lateral designs and resultant parasitic thermal conductance on the absolute accuracy of microcalorimeters based on a silicon-nitride membrane. Thermal properties are quantified by the curve fitting scheme based on the thermal relaxation method with two thermal decay times. In the studies of various microcalorimeter layouts, the temperature dependence of errors in the absolute values of heat capacity was found to be approximately proportional to that of the thermal conductance between the isothermal platform and the temperature reservoir. Decreasing parasitic thermal conductance by modifying the lateral designs for the thermometer and heater allowed for absolute accuracies that were typically less than 5% in a temperature range between 20 and 300 K.

1. Introduction

The heat capacity of solids provides basic information about the physical properties of materials, such as the electron and phonon densities of states [1], magnetic ordering [2–4], and structural and electronic phase transitions [5,6]. However, accurate heat capacity measurements are often complicated and limited by the measurement device, namely, the addenda heat capacity. If the heat capacity of the addenda is much larger than that of the sample, the measured sample heat capacity is likely to be subject to large errors and uncertainties. Furthermore, above 100 K, a common calorimeter platform made of a thin sapphire crystal exhibits a significant phonon specific heat contribution that is as high as $\sim 10^{-3}$–10^{-2} J/K; therefore, heat capacity measurements of a small-volume sample become increasingly challenging as temperature is raised. Increasing the sample quantity has been a traditional way of avoiding this problem. However, materials of interest often exist in a very small single-crystalline or thin-film form, whose heat capacity value only reaches a small fraction of the addenda heat capacity. Therefore, accurate measurements of small heat capacities by utilizing conventional calorimetry techniques can be quite challenging.

As an alternative approach, reducing the addenda heat capacity would be of great help. In fact, numerous efforts have been made to fabricate novel calorimeters with greatly reduced addenda heat capacity. The seminal development of microcalorimeters based on an amorphous silicon-nitride (Si-N) membrane was first reported by Denlinger et al. in 1994 [7]. Since then, many types of MEMS (Micro-Electro-Mechanical-Systems)-enabled microcalorimeters have been fabricated for measuring the heat capacity of various small-volume materials [8–11]. For example, qualitative changes in the heat capacity from melting transitions of sub-angstrom metal films can be determined using such a microcalorimeter [12]. In more recent developments, the specific heats of a few nanoliters of organic liquids [13] and biomaterials [14] have been measured by using a modified microcalorimeter platform.

However, to our knowledge, the quantitative accuracy of the heat capacity value has not been fully checked through the experimental efforts of using various types of microcalorimeters. Revaz et al. [15] have studied the accuracy of heat capacity measurements and its relationship with the thickness of the isothermal metal layer, mainly through numerical simulations. Other efforts to reduce measurement errors have been so far limited to the optimization of sample mass and temperature window [16]. Therefore, it is desirable to systematically check the accuracy of various microcalorimeters having different design parameters such as the shape of the heater and sensor and line widths of electrical leads. While it is possible to test the accuracy of various types of microcalorimeters through the measurements of a standard bulk material such as Cu, the experimental efforts toward the direction are scarce. This appears to be partly caused by the fact that as the addenda heat capacity decreases, the conventional relaxation

* Corresponding author.
E-mail addresses: parkyd@phya.snu.ac.kr (Y.D. Park), khkim@phya.snu.ac.kr (K.H. Kim).

0040-6031/$ – see front matter © 2008 Elsevier B.V. All rights reserved.
doi:10.1016/j.tca.2008.11.011

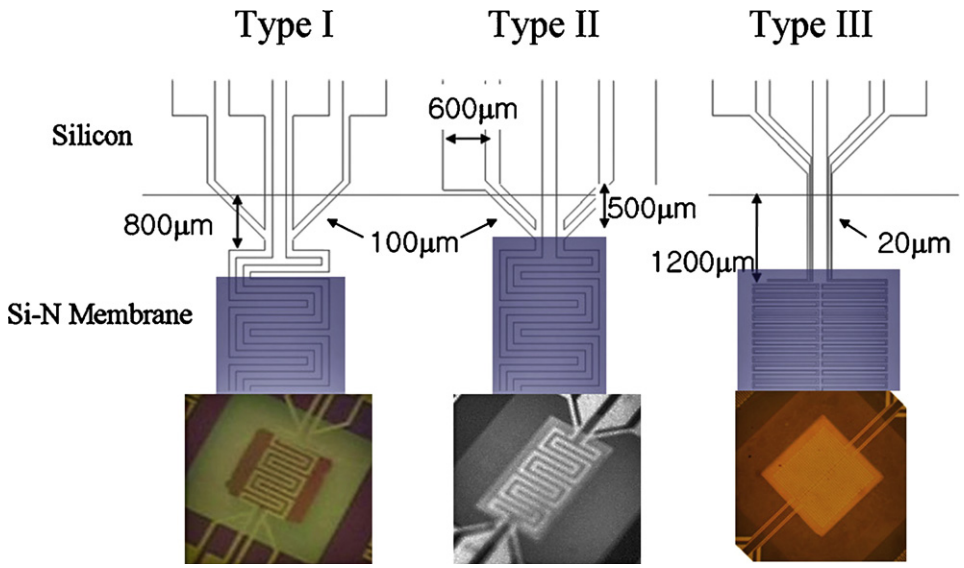

Fig. 1. Three different types of microcalorimeters were fabricated. As discussed in the text, based on results for types I and II, type III was designed to reduce λ_l by making the electrical leads narrower than those used in types I and II.

method with a single relaxation time loses more its accuracy as well as the measurement speed.

In this work, we have systematically studied the effects of various lateral designs and electrical line widths on the accuracy of the heat capacity measurements using Si-N-membrane-based microcalorimeters. By fabricating three different prototypes and employing a modified relaxation method with two relaxation time constants, called as the 'lumped-τ_2 model' in the original literature [17], we have achieved an accurate measurement scheme. A comparison of the thermal conductance of the electrical leads/Si-N membrane and the heat capacity data of a standard Cu sample from each microcalorimeter revealed that the heat loss and heat confinement are key factors affecting the accuracy of heat capacity data. When the thickness of each isothermal metal film and the membrane layer is more or less fixed, a heater/sensor layout with narrower electrical leads (width: 20 μm) provides accurate heat capacity data with errors less than 5% between 20 and 300 K. This observation suggests that in addition to thickness of the metal isotherm and the membrane [15], control of lateral design such as line width can be also important to achieve an isothermal condition in the membrane.

2. Fabrication of type III microcalorimeter

We used the general KOH etching method to fabricate three different types of Si-N-based microcalorimeters with different lateral and lead designs [11]. First, we deposit low-stress Si-N on the Si wafer using low-pressure chemical vapor deposition. The heater and the thermometer are defined using standard photolithographic techniques and metallization followed by lift-off. For the heater and thermometer, we use Au (types I and III) or Pt (type II) with a thickness of 50 nm. Cr or Ti (3 nm) is also used as an adhesion layer. After the lift-off, we form an etch mask on the opposite side using reactive ion etching. Then, the wafer is etched in a 20 wt% KOH solution, and the temperature is maintained at ~90 °C for 4 h. After this step, we deposit the isothermal layer on the Si-N membrane. The thickness of the isothermal region is ~200 nm with a Cr adhesion layer. The detailed fabrication techniques have been described in a previous report [11]. We note that as compared with the original procedure [7], the heater/sensor leads have been deposited before the KOH etching in our case. This reversed sequence has been quite useful in reducing the failure rate in the microfabrication processing.

Fig. 1 shows three different microcalorimeter designs. The heater/sensor film of type I is made of Au and has a uniform line width in the joint region while that of type II is made of Pt and has a line width that gradually decreases from the edge region toward the central region. In addition, the isothermal Au film of type I, which is gray in color in Fig. 1, had partially covered the heater/sensor regions while that of type II has tightly covered them. Thus, it is likely that the type II microcalorimeter has a better heat confinement to the isothermal layer. Both types I and II microcalorimeters are fabricated to have the same heater/sensor line width (thickness), 100 μm (50 nm), inside the isothermal layers. On the other hand, type III is designed to have much narrower electrical leads (line width: ~20 μm), see Fig. 1, and Au is used for the heater/sensor. Moreover, we made the heater and sensor regions well separated in our design to reduce the electrical interference between the heater and sensor leads through capacitive coupling. In order to use the four-probe method, every heater/sensor has four electrical leads. Table 1 summarizes line widths and thicknesses of the layers used in each type of microcalorimeter.

For the type III, in particular, the joint region of the heater and sensor lines is located well inside the isothermal region. This feature should be beneficial in determining the temperature of the isothermal layer more accurately. In addition, due to the same reason, applied power from the heater line in the isothermal layer can be also accurately determined. Moreover, the uniform and narrow linewidth of ~20 μm for the sensor and heaters enabled us to achieve quite a small λ_l value, which turns out to be useful in enhancing the accuracy as will be discussed in Section 4.

On the other hand, it is expected that the line width in the type III cannot be reduced indefinitely because the heater segment located in-between the isothermal layer and the heat reservoir regions can also generate heat. In our type III microcalorimeter, the relative ratio of the heater length outside and inside the isothermal layer is about 1:15, allowing the heat generated outside the isothermal region to be up to 6% of that inside. This extra heat is expected to be transferred to the heat sink, but it might also cause an erroneous power input or non-uniform temperature gradient to the isothermal region. Therefore, the reduction of the linewidth to achieve small λ_l might have to be compromised as well to mitigate the dissipation within the heater segment outside the isothermal layer.

We further note that the thickness of the metal layer is 200 nm for all the types of the microcalorimeter while the thickness of the

Table 1
Summary of layouts in the types I, II, and III microcalorimeters.

	Type I	Type II	Type III
Heater/sensor thickness	Au: 50 nm; Ti: 3 nm	Pt: 50 nm; Ti: 3 nm	Au: 50 nm; Cr: 3 nm
Heater/sensor width	100 μm	100 μm	20 μm
Isothermal layer thickness	Au/Ti: 200 nm	Au/Ti: 200 nm	Au/Cr: 200 nm
Si-N membrane thickness	950 nm	750 nm	1000 nm

membrane has some variation. From the ellipsometry study, the thickness of the membrane is found to be 950, 750, and 1000 nm for types I, II, and III microcalorimeter, respectively. Errors of the ellipsometry measurement were ±10 nm. Thus, the thickness ratio of the membrane and metallic layers varies from 4:1 to 5:1. We find that this particular choice of a rather thick membrane is advantageous because we can achieve very high production yields; from a 4 in. Si wafer, we can get 37 devices without breaking any of the membrane platforms. However, the production yields for the thinner membrane with ~200 nm thickness became much lower. Moreover, the microcalorimeter with the thicker membrane can be reused more. Therefore, we have chosen ~1000 nm for the membrane thickness in the type III microcalorimeter to be the optimal thickness. In Section 4, we will further discuss how the specific choice of the membrane thickness can affect the accuracy.

3. Heat capacity measurement scheme

In order to characterize these microcalorimeters, we used a Physical Property Measurement System (PPMS, Quantum Design) and a customized program based on the thermal relaxation model with the two relaxation times, i.e., the lumped-τ_2 model [17]. Recently, stressing the least-square-fitting scheme in the application of the lumped-τ_2 model, Hwang et al. [18] have called the fitting scheme as the "curve fitting model (CFM)", which terminology has been also used in our previous work [11]. In fact, the commercial heat capacity option in PPMS employs a similar least-square-fitting scheme with two relaxation times. Moreover, the accuracy of the commercial scheme using a sapphire platform has been verified by Lashley et al. [19].

To test various types of microcalorimeters, we have developed a customized program with LabVIEW™ based on the above curve fitting scheme. The distinctive feature of our scheme compared to the commercial one is in the use of a commercial lock-in amplifier to measure the sensor resistance at a frequency of ~2 kHz. The resistance measured with a lock-in time constant of 3–10 ms is recorded with a sampling rate of 2–256 points/s. The actual sampling rate can be automatically selected in each measurement to cover the relaxation time of the sample investigated. The relaxation time we measure can be as short as 50 ms. This fast measurement scheme is advantageous for measuring small heat capacity of the addenda as well as the micrometer-sized samples using the microcalorimeter.

The curve fitting scheme based on the lumped-τ_2 model [11,18] assumes that a finite thermal conductance exists between the sample and the isothermal layer, in addition to that between the isothermal layer and the outside thermal reservoir (Fig. 2(a)). In this case, internal thermal conductance of the sample investigated is assumed to be infinite. The temperature of a reservoir block, T_0, is controlled by the PPMS. If we assume that, initially, the T_0 is constant and is in equilibrium with the sensor temperature T, the general heat transfer equations can be expressed as

$$\begin{aligned} P(t) &\equiv c'\frac{dT'}{dt'} + \lambda_s(T' - T) + \lambda_l(T' - T_0) \\ 0 &= c\frac{dT}{dt} + \lambda_s(T - T') \end{aligned} \tag{1}$$

where P, c, c', λ_l, and λ_s denote applied power, heat capacity of the sample, heat capacity of the platform, thermal conductance between the membrane platform and the thermal reservoir, and thermal conductance between the sample and the isothermal platform, respectively. Following the procedure in Ref. [18], Eq. (1) can be modified to express the temperature change in the isothermal region, $\Gamma(t) \equiv T'(t) - T'(t)$, in the form of a linear combination of $H(t)$,

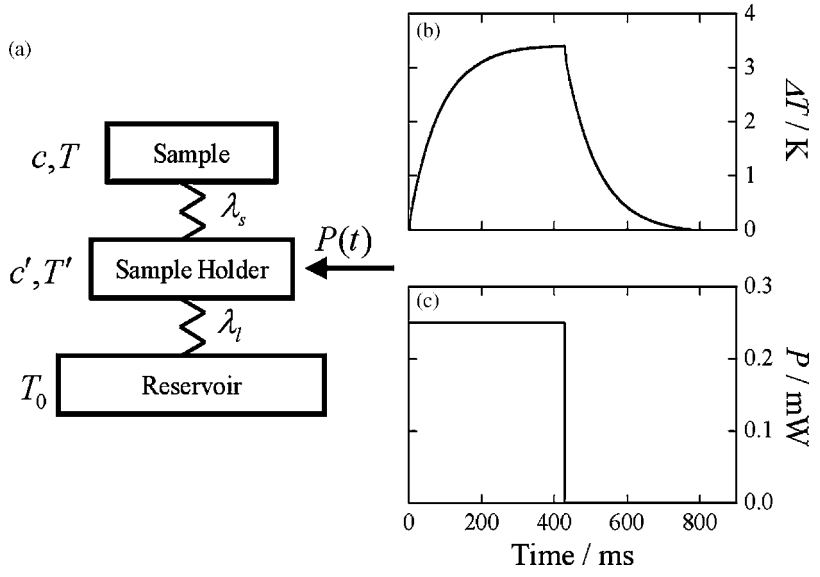

Fig. 2. (a) The used thermal relaxation model, considering the finite thermal conduction between the sample and the isothermal region of the microcalorimeter (λ_s), called also as the lumped-τ_2 model [17]. (b) Time-dependent temperature response (ΔT) of the microcalorimeter to the (c) applied heating power (P). Based on these experimental curves, $\Gamma(t)$, $H(t)$, $Q(t)$, and $S(t)$ defined in Eq. (2) are extracted, and the sample heat capacity, λ_l, and other parameters shown in (a) can be obtained from the curve fitting method as explained in texts.

$S(t)$, and $Q(t)$

$$\Gamma(t) \equiv \frac{c/\lambda_s}{c' + c + c(\lambda_l/\lambda_s)} H(t) + \frac{-\lambda_s}{c' + c + c(\lambda_l/\lambda_s)} S(t) + \frac{1}{c' + c + c(\lambda_l/\lambda_s)} Q(t) \quad (2)$$

where $H(t) \equiv P(t) - c'(dT'/dt'|_{t'=t} - dT'/dt'|_{t'=0})$, $S(t) \equiv \int_0^t T'(t')dt'$ and $Q(t) \equiv \int_0^t P(t')dt'$. Here, $\Gamma(t)$, $H(t)$, $Q(t)$, and $S(t)$ can be calculated from the experimentally measured data, i.e., heater power and sensor temperature, as shown in Fig. 2(b). A DC current is applied to the heater through a source meter, which also records the applied voltage to calculate the total power $P(t)$. Since Eq. (2) holds in each n-th time-segment (t_n) when the sensor temperature is recorded, it constitutes n-independent equations with each experimentally available variable $\Gamma(t_n)$, $H(t_n)$, $Q(t_n)$, and $S(t_n)$. In practice, we have digitized the temperature-variation of the sensor with a time resolution of approximately 10 ms to record more than 100–2000 points during one typical measurement cycle of 1–20 s. The measurement time can be selected to be proportional to the actual relaxation time of the sample at each temperature, which typically corresponds to 0.3–10 s for the type III microcalorimeter below 300 K. By employing the least-square-fitting scheme over the n-independent experimental variables $\Gamma(t_n)$, $H(t_n)$, $Q(t_n)$, and $S(t_n)$, three constant coefficients in front of $H(t)$, $Q(t)$, and $S(t)$ in Eq. (2) can be determined at each temperature. Then, using the predetermined c' values from the addenda measurement, we can determine the remaining unknown parameters, c, λ_l, and λ_s [18]. The finite value of λ_s obtained by the fits to the data means that the CFM corrects the so-called "τ_2 effect", which is caused by a finite thermal conductance between the sample and the membrane platform.

The above curve fitting scheme based on the two relaxation times constitutes a crucial advantage over the conventional relaxation method; for small single-crystalline samples, for example, a good thermal contact with the membrane platform cannot be easily achieved due to the high fragility of the thin membrane under pressure. Even if thermal grease is used, the thermal contact between a sample and a membrane platform often turned out to be poor. Therefore, according to our experience, the conventional relaxation method using a single decay time gives rise to significant errors. More importantly, we find that the above CFM becomes quite useful in tracking down the error source in the use of our microcalorimeters (*vide infra*), because it can effectively correct the errors from the "τ_2 effect" and produce reliably above three independent parameters c, λ_l, and λ_s. More details about the measurement scheme based on the types I and II microcalorimeters can be also found in a previous publication [11].

4. Results

In order to check the accuracy of the microcalorimeter, we have investigated the specific heat of oxygen-free-high-conducting-copper. A small piece of Cu (~300 μg) was attached to the isothermal platform of a microcalorimeter by using N-grease (Apiezon) as thermal grease. Then, the microcalorimeter was installed in the PPMS cryostat. Before measuring the Cu specimen, the addenda heat capacity including the isothermal platform and the thermal grease was measured. At each temperature, the addenda heat capacity was automatically subtracted from the acquired data to calculate the heat capacity of Cu (Fig. 3(a)). Fig. 3(b) shows that for types I and II, measurement errors were as large as 30% as compared to the standard Cu specific heat [20] and thus both types of microcalorimeters were found to produce rather inaccurate values of specific heat.

While inspecting other measured parameters, we found that the overall temperature dependence of the measurement errors

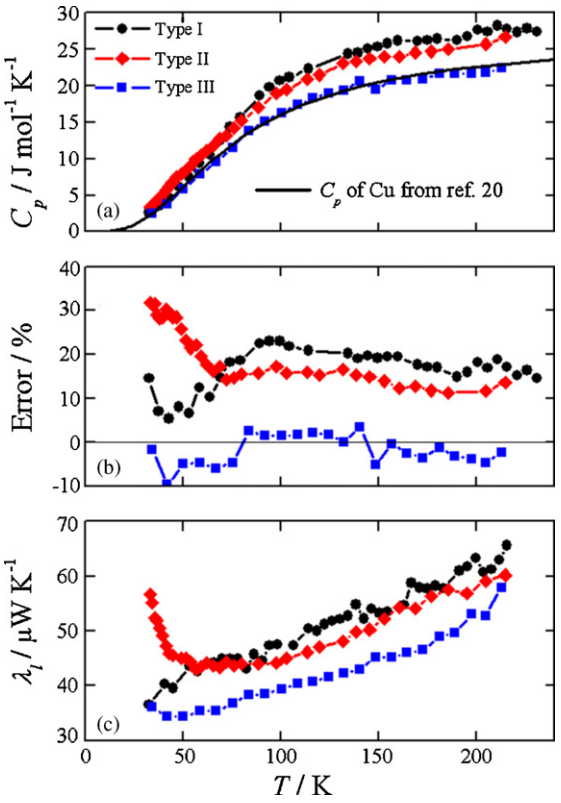

Fig. 3. Measurement results obtained using three types of microcalorimeters (circles, diamonds, and squares represent types I, II, and III, respectively): (a) Specific heat of Cu measured using types I, II, and III. Results obtained using type III are in good agreement with the reference data (solid line). (b) Errors in the Cu specific heat measurements using the microcalorimeters. Type III exhibits the smallest error of approximately ±5%. (c) λ_l of each microcalorimeters. Note that type III exhibits the smallest λ_l value at all temperature range.

exhibits a similar behavior to the temperature dependence of λ_l of the devices in both types I and II (see, Fig. 3(b) and (c)). Even the magnitudes of the errors increased in correlation to the magnitude of λ_l in both types I and II microcalorimeters. Therefore, we can presume that a large value of λ_l might cause an unwanted thermal gradient in the isothermal region. This parasitic effect can cause an underestimation of the temperature for the isothermal platform. The underestimation of the temperature under the same heat power will result in a heat capacity value that is apparently larger than the real one. This can explain why the measured specific heat of Cu is larger than that given in the reference data. Furthermore, these results directly imply that careful control of λ_l is critical for enhancing the measurement accuracy of the microcalorimeter.

In order to overcome the temperature underestimation in the isothermal region, there can be at least two kinds of solution, i.e., reducing λ_l to have better heat confinement to the isothermal layer and increasing thickness of the metallic isothermal layer to have better isothermal condition. The latter condition can be reached by increasing the thickness of the Au isotherm layer to reach almost a comparable thickness of the Si-N membrane, i.e., ~1 μm [15]. However, a significant increase in the Au isotherm thickness is detrimental since the addenda heat capacity increases correspondingly. Moreover, our efforts to fabricate a thick Au film resulted in an increased probability of being detached from the Si-N membrane. This effect appears to be caused by increased Au film stress during a longer deposition thermal cycling. On the other hand, as we have targeted to fabricate rather a robust microcalorimeter for repeated usages, the other approach of reducing thickness of the Si-N membrane has not been tried.

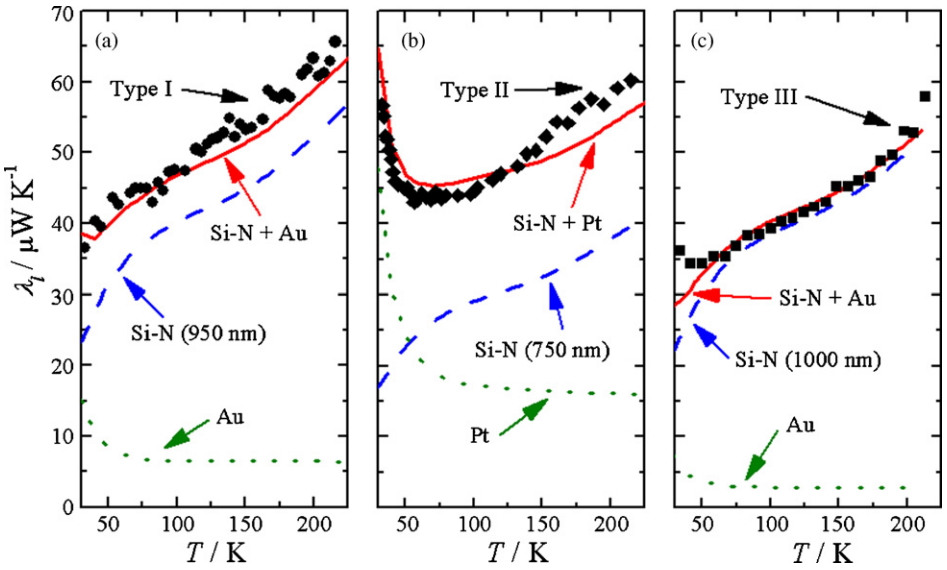

Fig. 4. Comparison between experimentally determined λ_l (symbols) and the theoretical estimation (solid lines) of each (a) type I, (b) type II, and (c) type III. Dotted and dashed lines represent the thermal conductance of the metal leads and the Si-N membrane, respectively. To calculate the metal lead contribution, the number of leads, thickness, and width are multiplied with the thermal conductivity of each metal [20]. The contribution of Si-N is estimated from the thermal conductivity data [21] multiplied by its thickness and the 2D geometrical factor $\alpha = 20$ (see texts for details).

Instead, we have tried to reduce λ_l by reducing the metallic leads contribution because the lateral dimension of them can be more easily adjusted without affecting the fabrication yields. Fig. 4 shows the experimentally determined (symbols) and theoretically estimated (lines) λ_l for three types of microcalorimeters (those for types I and II are replotted from Ref. [11]). Here, $\lambda_l(T) \equiv \lambda_{leads}(T) + \lambda_{Si\text{-}N}(T)$ where $\lambda_{leads}(T)$ and $\lambda_{Si\text{-}N}(T)$ are contribution of electrical leads and Si-N, respectively. $\lambda_{leads}(T)$ was calculated from the reported data of each material [20] and its dimension. For calculation of $\lambda_{Si\text{-}N}(T)$, thermal conductivity value for an amorphous Si-N film [21] was multiplied by our film thickness and a 2D geometrical factor α. After combining both $\lambda_{leads}(T)$ and $\lambda_{Si\text{-}N}(T)$, calculated $\lambda_l(T)$ was fitted to the experimental data by setting α as the free fitting parameter [11] The optimal fitting value of α was 20 in our case while $\alpha = 10$ in refs. [7] and [15], indicating thermal conductivity of our Si:N film is larger by a factor 2 than that in Refs. [7] and [15].

We find that in Fig. 4, the thermal conductance of the electrical leads contributes rather significantly to the total λ_l. For the type II microcalorimeter (Fig. 4(b)), the contribution of the electrical leads remains ~25% of the total λ_l above 75 K and reaches more than 50% below 75 K. For the type I (Fig. 4(a)), the contribution remains ~10% above 50 K and reaches more than 25% below. Thus, in both calorimeters, the thermal conductance of the metallic leads over that of the Si-N membrane is not negligible. The relative contribution is expected to become more significant when the thickness of the Si-N membrane reduces. More importantly, we notice that for each types I and II microcalorimeter, the temperature dependence of the errors in Fig. 3(b) was very similar to that of the metallic leads shown in Fig. 4. This observation suggests that the

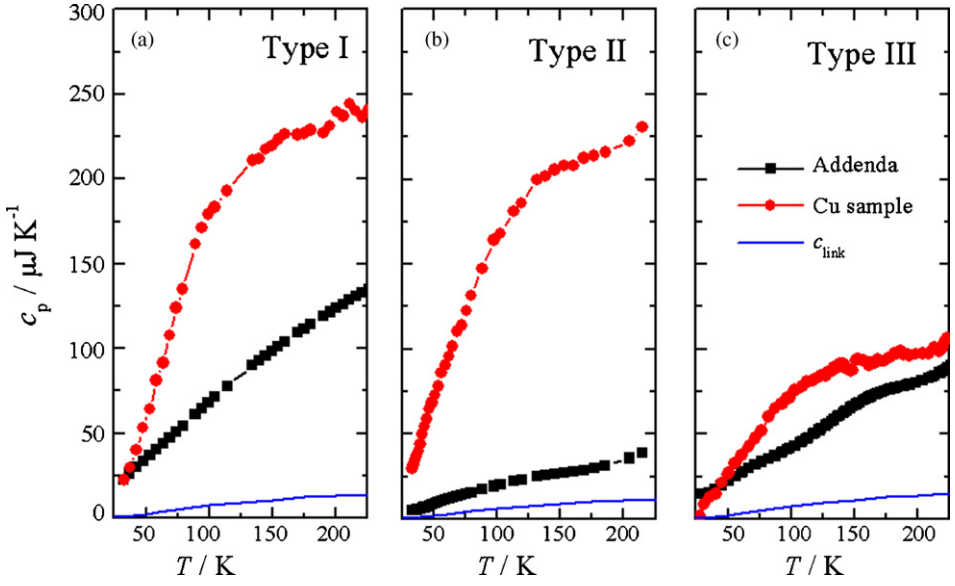

Fig. 5. Heat capacity data of addenda, Cu, and the wire (c_{link}) for three types of microcalorimeters. Au was used as electrical leads for types I and III, while Pt was used for type II.

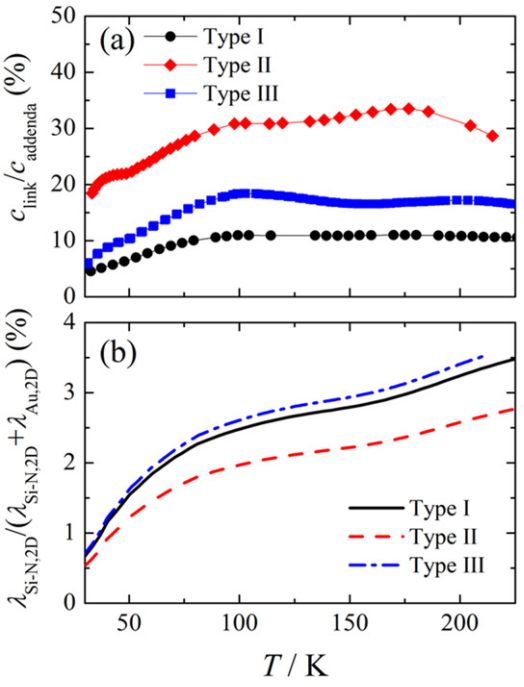

Fig. 6. Calculated (a) $c_{link}/c_{addenda}$ and (b) $\lambda_{Si\text{-}N,2D}/\lambda_{platform,2D} \equiv \lambda_{Si\text{-}N,2D}/(\lambda_{Si\text{-}N,2D}+\lambda_{Au,2D})$ for the three types of microcalorimeter. Here, $\lambda_{2D} = \kappa \times$ (thickness), in which κ data for Au and Si-N, respectively [20,21]. Considering that our Si-N membrane might have larger thermal conductance by two times than that in previous works [7,15], the ratio given in (b) can be doubled.

larger thermal conductance of the metallic leads can result in the larger errors. Thus, we postulated that reducing thermal conductance contribution of metallic leads can be a first necessary step to improve the accuracy. At the same time, a better heat confinement to the isotherm, which should be useful for reducing the thermal gradient in the membrane, can be also achieved by increasing relative length of the heater lines.

Based on these reasonings, we have designed the type III microcalorimeter that has much narrower electrical leads with a width of 20 μm and has longer heater lines. Moreover, as compared with types I and II, its heater/sensor section is well located inside the Au film region. Thus, the type III microcalorimeter is expected to have better heat confinement and more accurate temperature reading. This approach has provided an additional advantage for heat capacity measurements using the CFM. The thermal relaxation time at each temperature is roughly equal to the heat capacity of a specimen over thermal conductance λ_l. It is unavoidable to have a small heat capacity of a specimen in a microcalorimeter by a factor of ~10–1000 over the conventional calorimeter. Without reducing λ_l, the relaxation time then may become too short for measurements using conventional instruments. Thus, an increase in the intrinsic relaxation time by reducing λ_l can be quite useful for increasing the number of digitized signals, thus enhancing the accuracy of the fit. Therefore, we conclude that reducing λ_l via the narrower electric leads will make relaxation times increase and thus will provide a better chance for achieving accurate measurements in the relaxation method.

The heat capacity data of the Cu specimen from the type III microcalorimeter has become more accurate than that obtained from the types I and II devices, as demonstrated in Fig. 3(b). Furthermore, Fig. 3(c) proves that λ_l of type III becomes much smaller than that of types I and II. Analyses of each contribution to λ_l of type III, as seen in Fig. 4(c), also reveal that the thermal conductance of Au wires indeed reduces significantly as expected. Using the type III, the accuracy of measurements is within approximately ±5% between 20 and 300 K. Moreover, even when we measure the Cu specimen with a different mass, the accuracy still remained intact for the mass ranges from ~50 to 1000 μg. Although a 20% smaller value of λ_l, as shown in Figs. 3(c) and 4(c), can make the time constant rather longer, the total measurement time did not increase significantly. This is because the CFM only requires a short measurement time approximately twice that of the thermal relaxation time. Therefore, our results show that a proper engineering of λ_l via much narrower metallic leads or confined heater region can be useful for acquiring accurate heat capacity data on samples of typical mass ~10–1000 μg in the use of the Si-N microcalorimeter.

5. Discussions

A caveat in applying the lumped-τ_2 model for extracting heat capacity is the fact that it assumes the 1D heat transfer while the thermal flow in the microcalorimeter is governed by 2D heat transfer in practice. Therefore, to apply the above 1D model into the microcalorimeter, one still needs to check several conditions. The conditions for applying the 1D thermal relaxation model have been discussed in the work of Bachmann et al. [17]. The first condition is related to the ratio between heat capacity of the outside link and the isothermal layer. Specifically, when $c_{link}/(c_{addenda}+c_{sample}) < 0.1$, the total heat capacity measured $(c_{addenda}+c_{sample})$ can contain $1/3c_{link}$ within the accuracy of 1%. In our measurements, we have measured $c_{addenda}$ first, and then put a sample into the platform to measure total heat capacity. Then, c_{sample} was obtained by subtracting $c_{addenda}$ from the total heat capacity. In this subtraction process, if the contribution from the thermal link is approximately constant as $1/3c_{link}$, c_{sample} can become accurate. To check this, we have plotted the experimental $c_{addenda}$, c_{Cu}, and estimated c_{link} for each microcalorimeter in Fig. 5. Here, $c_{link} = V_{Si\text{-}N} \times \rho_{Si\text{-}N} \times C_{Si\text{-}N} + V_{leads} \times \rho_{leads} \times C_{Au/Pt}$, in which V, ρ, and C stand for volume, density, and specific heat of each material, respectively. For Si-N contribution to the heat capacity, known specific heat of $c_{Si\text{-}N}$ [21] was used. In each case, we can find the c_{link} is quite smaller than c_{Cu} and $c_{addenda}$. The actual ratio of $c_{link}/c_{addenda}$ plotted in Fig. 6(a) is more or less around 10%, for both types I and III. The $c_{link}/c_{addenda}$ ratio of ~10% suggests that the condition by Bachmann et al. [17] is valid and the measurement is accurate within ~1%. Even if $c_{link}/c_{addenda}$ reaches around 30% for type II, we notice that the measurements errors of type II in Fig. 2(b) was even smaller at high temperature region than those of the type I. Therefore, $c_{link}/c_{addenda}$ ratio does not seem to be a deciding factor for the accuracy of the measurement.

Another condition one should check before applying the 1D lumped-τ_2 model is whether $\lambda_l/\lambda_{platform} \ll 1$. Although the λ_l is determined experimentally in Fig. 3 for each type, this should be an effective 1D thermal conductance of the link. Moreover, the effective 1D $\lambda_{platform}$ is not easy to determine experimentally. In Ref. [15], the validity of the 1D relaxation model in the application of the microcalorimeter has been checked numerically for various 2D thermal conductance ratios between the isothermal platform, composed of the Si-N membrane and the metal isotherm, and the Si-N membrane layer. The 2D thermal conductance of each layer is defined as the multiplication of thickness and thermal conductivity (κ) of the material used; $\lambda_{Si\text{-}N,2D} \equiv t_{Si\text{-}N}\,\kappa_{Si\text{-}N}$, and $\lambda_{platform,2D} \equiv \lambda_{Si\text{-}N,2D} + \lambda_{Au,2D} = t_{Si\text{-}N}\,\kappa_{Si\text{-}N} + t_{Au}\,\kappa_{Au}$. When $\lambda_{platform,2D}/\lambda_{Si\text{-}N,2D} = 100\text{–}50$, isothermal condition of the platform was nearly achieved (Fig. 2 in Ref. [15]) and the 1D model is then valid with errors less than 1% (Fig. 8(c) in Ref. [15]). Even if the ratio $\lambda_{platform,2D}/\lambda_{Si\text{-}N,2D}$ becomes close to 10, the deviations remained less than 4%.

In our case, given the geometry of each calorimeter, we have calculated the ratio $\lambda_{Si\text{-}N,2D}/\lambda_{platform,2D}$ in Fig. 6(b), using the thermal conductivity of both Au and Si-N available in the literatures [20,21].

For each calorimeter, $\lambda_{Si\text{-}N,2D}/\lambda_{platform,2D}$ is always less than 3% at temperatures below 300 K, and gets smaller down to around 1% as we further decrease temperature to 20 K. Therefore, each type of microcalorimeter has $34 < \lambda_{platform,2D}/\lambda_{Si\text{-}N,2D} < 100$. If we refer to the numerical simulation results [15], the errors caused by this effect is close to 1%. Therefore, the thermal conductance ratio of $\lambda_{platform,2D}/\lambda_{Si\text{-}N,2D}$ indicates that each microcalorimeter is mostly within the valid 1D regime, suggesting that $\lambda_{platform,2D}/\lambda_{Si\text{-}N,2D}$ is not a deciding factor for the error shown in Fig. 3(c) either. This conclusion is also supported by the fact that the errors appeared in Fig. 3(b) are not directly proportional to the magnitude of $\lambda_{platform,2D}/\lambda_{Si\text{-}N,2D}$ in Fig. 6(b). Thus, a main error source in the types I and II seems to be more directly related to λ_l, as discussed in Section 3.

On the other hand, our previous study [11], and analyses in Fig. 4, has revealed that the thermal conductivity of the Si-N membrane in the types I and II is larger by a factor of two than that of a typical Si-N membrane [7,15]. In Fig. 4(c), the thermal conductance of the Si-N membrane for type III is also comparable to that of type I (Fig. 4(a)) so that thermal conductivity of the type III is also expected to be larger by a factor of two than that in Refs. [7] and [15]. It is postulated that the thermal conductivity of our membrane is enhanced with its increased thickness, presumably due to its lowered stress. If this is the case, the value of $\lambda_{Si\text{-}N,2D}/\lambda_{platform,2D}$ in Fig. 6(b) should be approximately doubled, yielding $17 < \lambda_{platform,2D}/\lambda_{Si\text{-}N,2D} < 50$ at overall temperatures. According to Ref. [15], these values of $\lambda_{platform,2D}/\lambda_{Si\text{-}N,2D}$ then can give rise to errors in the application of the 1D model up to about 4%. Then, the intrinsic errors of type III around 5% might be a natural consequence of the larger thermal conductance of the Si-N layer that results in a poor heat confinement into the isothermal layer and thus makes the 1D thermal modeling imperfect. It should be also possible that the errors observed in the types I and II microcalorimeters are amplified due to this rather imperfect isothermal condition imposed by the specific $\lambda_{platform,2D}/\lambda_{Si\text{-}N,2D}$ ratio of the microcalorimeter. Therefore, the results presented here should not be interpreted as implying that the original design in Refs. [7,15] has errors in the absolute heat capacity. Furthermore, reducing the membrane thickness with the same lateral designs as type III is expected to enhance the accuracy further while it can generate less strong membrane platform. The parallel effort of performing the 2D heat transfer simulation can be also desirable in the type III microcalorimeter to explore a proper design direction that can further enhance the accuracy.

6. Conclusion

In summary, we have fabricated three different microcalorimeters having different λ_l values by changing the design of the electrical leads and lateral layouts. By determining a systematic relationship between the measurement error and λ_l, we have shown that λ_l should be properly engineered to enhance the accuracy of heat capacity measurements using the Si-N-membrane-based microcalorimeter and the 1D thermal relaxation method. Our findings imply that one design direction for achieving a more enhanced accuracy is to reduce the heat loss through electrical leads and to confine heat in the isothermal platform. Therefore, efforts to achieve narrower line width and smaller heater and sensor region are expected to result in a microcalorimeter with more enhanced accuracy. Furthermore, our investigations show that employing the curve fitting method can be useful for experimentally determining heat capacity as well as estimating the accuracy of various types of microcalorimeter. Computer simulations based on finite element analyses would be desirable to further enhance the performance of our type III microcalorimeter.

Acknowledgements

We thank Professor Greg Stewart for the critical reading of the manuscript and D.H. Nam for helps in the experiment. We are supported by the Seoul R&BD program. KHK further acknowledges support from the National Research Lab Program (M10600000238) and the KICOS grant (K20702020014-07E0200-01410) provided by the MEST.

References

[1] J.E. Lorenzo, R. Currat, A.J. Dianoux, P. Monceau, E. Levy, Phys. Rev. B 53 (1996) 8316.
[2] F. Bouquet, Y. Wang, I. Sheikin, T. Plackowski, A. Junod, S. Lee, S. Tajima, Phys. Rev. Lett. 89 (2002) 257001.
[3] J. Konig, H.H. Lin, A.H. MacDonald, Phys. Rev. Lett. 84 (2000) 5628.
[4] P.A. Sharma, J.S. Ahn, N. Hur, S. Park, S.B. Kim, S. Lee, J.G. Park, S. Guha, S.W. Cheong, Phys. Rev. Lett. 93 (2004) 177202.
[5] K.R. Juraitis, J.B. Domiciano, W. Sano, Phys. Rev. B 42 (1990) 2586.
[6] V.N. Smolyaninova, K. Ghosh, R.L. Greene, Phys. Rev. B 58 (1998) R14725.
[7] D.W. Denlinger, E.N. Abarra, K. Allen, P.W. Rooney, M.T. Messer, S.K. Watson, F. Hellman, Rev. Sci. Instrum. 65 (1994) 946.
[8] S.G. Doettinger-Zech, M. Uhl, D.L. Sisson, A. Kapitulnik, Rev. Sci. Instrum. 72 (2001) 2398.
[9] S.L. Lai, G. Ramanath, L.H. Allen, P. Infante, Z. Ma, Appl. Phys. Lett. 67 (1995) 1229.
[10] Y.Y. Zhang, S. Tadigadapa, Appl. Phys. Lett. 86 (2005) 034101.
[11] K.S. Suh, H.J. Kim, Y.D. Park, K.H. Kim, S.W. Cheong, J. Korean Phys. Soc. 49 (2006) 1370.
[12] M. Zhang, M.Y. Efremov, E.A. Olson, Z.S. Zhang, L.H. Allen, Appl. Phys. Lett. 81 (2002) 3801.
[13] E.A. Olson, M.Y. Efremov, A.T. Kwan, S. Lai, V. Petrova, F. Schiettekatte, J.T. Warren, M. Zhang, L.H. Allen, Appl. Phys. Lett. 77 (2000) 2671.
[14] Z.S. Zhang, O.M. Wilson, M.Y. Efremov, E.A. Olson, P.V. Braun, W. Senaratne, C.K. Ober, M. Zhang, L.H. Allen, Appl. Phys. Lett. 84 (2004) 5198.
[15] B. Revaz, B.L. Zink, D. O'Neil, L. Hull, F. Hellman, Rev. Sci. Instrum. 74 (2003) 4389.
[16] B. Revaz, B.L. Zink, F. Hellman, Thermochim. Acta 432 (2005) 158.
[17] R. Bachmann, F.J. DiSalvo Jr., T.H. Geballe, R.L. Greene, R.E. Howard, C.N. King, H.C. Kirsh, K.N. Lee, R.E. Schwall, H.-U. Thomas, R.B. Zubeck, Rev. Sci. Instrum. 43 (1972) 205.
[18] J.S. Hwang, K.J. Lin, C. Tien, Rev. Sci. Instrum. 68 (1997) 94.
[19] J.C. Lashley, M.F. Hundley, A. Migliori, J.L. Sarrao, P.G. Pagliuso, T.W. Darling, M. Jaime, J.C. Cooley, W.L. Hults, L. Morales, D.J. Thoma, J.L. Smith, J. Boerio-Goates, B.F. Woodfield, G.R. Stewart, R.A. Fisher, N.E. Phillips, Cryogenics 43 (2003) 369.
[20] D.R. Lide (Ed.), CRC Handbook of Chemistry and Physics, CRC Press, Boca Raton, 2004.
[21] B.L. Zink, F. Hellman, Solid State Commun. 129 (2004) 199.